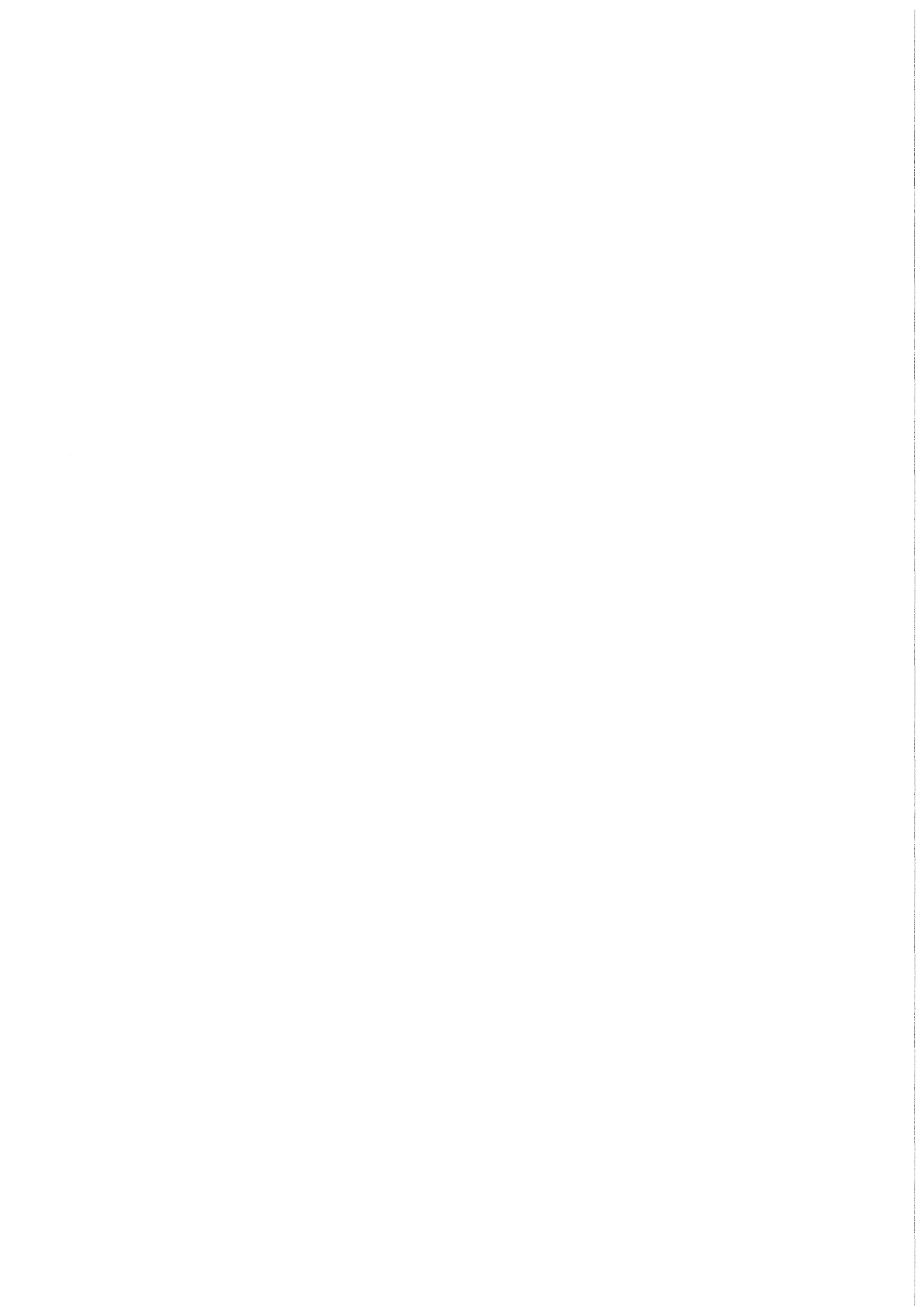


**KfK 4082  
Mai 1986**

# **On the Numerical Integration of Viscoplastic Models**

**V. K. Arya, K. Hornberger, H. Stamm  
Institut für Material- und Festkörperforschung**

**Kernforschungszentrum Karlsruhe**



KERNFORSCHUNGSZENTRUM KARLSRUHE  
Institut für Material- und Festkörperforschung

KfK 4082

On the numerical integration of  
viscoplastic models.

V.K. Arya\*, K. Hornberger and H. Stamm

KERNFORSCHUNGSZENTRUM KARLSRUHE GMBH, KARLSRUHE

---

\* Presently on leave from University of Roorkee, ROORKEE - 247 667, India.

Als Manuskript vervielfältigt  
Für diesen Bericht behalten wir uns alle Rechte vor

Kernforschungszentrum Karlsruhe GmbH  
Postfach 3640, 7500 Karlsruhe 1

ISSN 0303-4003

## ZUR NUMERISCHEN INTEGRATION VISKOPLASTISCHER MATERIALMODELLE

Mehrere explizite Integrationsmethoden wurden hinsichtlich ihrer Effektivität bei der Integration nichtlinearer "steifer" konstitutiver Gleichungen für viskoplastische Materialmodelle kritisch überprüft. Es zeigt sich, daß eine einfache Euler-Vorwärts Methode mit automatischer Schrittweitensteuerung gute Ergebnisse liefert. Die Möglichkeiten verschiedener Verfahren zur Schrittweitensteuerung wurden überprüft. Dabei hängt die erfolgreiche Anwendung eines Verfahrens - eines wird in diesem Bericht vorgestellt, ein anderes wurde von Kumar et al. vorgeschlagen - von dem zu integrierenden viskoplastischen Modell ab.

## ON THE NUMERICAL INTEGRATION OF VISCOPLASTIC MODELS

### Abstract

A critical examination of several explicit integration methods, for their effectiveness in the integration of nonlinear and stiff constitutive equations of viscoplastic models, has been presented. The use of a simple Euler-forward method with an automatic time step control strategy is seen to be encouraging. The capabilities of several such time step control strategies have been assessed. The success of integration strategy - one presented in the report and the other proposed by Kumar et al. - depends on the particular viscoplastic model being integrated.

## TABLE OF CONTENTS

	<u>Page</u>
LIST OF TABLES .....	ii
LIST OF FIGURES .....	iii
1. INTRODUCTION .....	1
2. VISCOPLASTIC MODELS (UNIAXIAL FORMS) .....	2
2.1 Bodner-Partom Model .....	2
2.2 Robinson Model .....	3
2.3 Walker Model .....	4
3. NUMERICAL INTEGRATION METHODS .....	5
3.1 Comparison of Integration Methods .....	6
4. INTEGRATION STRATEGIES WITH AUTOMATIC TIME-STEP CONTROL .....	9
4.1 Automatic Time-Step Control Integration Strategies Based on Taylor's Expansion .....	9
4.2 Integration Strategy Proposed By Kumar et al. ....	10
4.3 Present Integration Strategy .....	12
5. DISCUSSIONS .....	14
5.1 Bodner-Partom Model .....	14
5.2 Robinson Model .....	15
5.3 Walker Model .....	16
6. CONCLUSIONS .....	16
ACKNOWLEDGEMENTS .....	17
REFERENCES .....	18

LIST OF TABLES

<u>Table</u>		<u>Page</u>
I	MATERIAL CONSTANTS .....	23
	I(a). Bodner-Partom Model .....	23
	I(b). Robinson Model .....	23
	I(c). Walker Model .....	23
II	FORMULAE FOR NUMERICAL INTEGRATION METHODS .....	24
III	VALUES OF STRESS AT DIFFERENT TIMES (STRAINS) ....	26
	III(a). Bodner-Partom Model .....	26
	III(b). Robinson Model .....	27
	III(c). Walker Model .....	28
IV	VALUES OF STRESS OBTAINED USING THE INTEGRATION STRATEGIES PROPOSED (i) BY KUMAR et al. AND (ii) PRESENT REPORT	30
	IV(a). Bodner-Partom-Model .....	30
	IV(b). Robinson Model .....	31
	IV(c). Walker Model .....	33
V	COMPARISON OF ERROR NORMS AND CPU-TIMES .....	35

LIST OF FIGURES

<u>Figure</u>		<u>Page</u>
1	CYCLIC LOADING FOR DIFFERENT MODELS .....	36
	1(a). Bodner-Partom Model .....	36
	1(b). Robinson Model .....	36
	1(c). Walker Model .....	36
2-4	STRESS (ACCURATE) VERSUS STRAIN;POINTS FOR COMPARISON OF INTEGRATION STRATEGY .....	37-42
	2(a), 3(a), 4(a)-Kumar et al. Integration Strategy..	37, 39, 41
	2(b), 3(b), 4(b)-Present Integration Strategy .....	38, 40, 42

## 1. Introduction

The need for incorporating the influence of inelastic material behaviour into high-temperature design procedures for Nuclear Reactors and Gas-Turbine engines is now well recognized. The conventional way of treating the strain as the sum of a time independent component (plastic strain) and a time dependent component (creep strain) seems unjustified as only the combined effect is measurable. The necessity and importance of viscoplastic models, which treat the strain as a unified quantity, without artificially separating it into plastic and creep components, should thus be evident. During the last several years, considerable effort has, therefore, been devoted to the development of viscoplastic models to characterize the inelastic behaviour of materials under thermomechanical loadings at elevated temperatures. As a result a number of viscoplastic models has emerged and is available in literature [1-16]. The predicting capabilities of these models are different but each of these models is capable of predicting several of the following physical phenomena:

1. Behaviour in tension (loading/ unloading),
2. Behaviour in compression (loading/ unloading),
3. Initial elastic behaviour,
4. Creep,
5. Relaxation,
6. Rate sensitivity,
7. Anelasticity,
8. The Bauschinger effect,
- and 9. Cyclic hardening/ softening.

The viscoplastic models give a better representation of material behaviour, but the difficulty coupled with their use is that the constitutive differential equations associated with these models are highly nonlinear and "stiff" (used in a mathematical sense) to yield, in general, an analytical solution. Fortunately, the availability of versatile numerical methods such as the Finite-Difference, the Finite-Element or the Boundary Element methods, and of the high speed and large computers has facilitated the applicability of the viscoplastic models to the problems involving the high-temperature inelastic behaviour of materials.

Although some investigations using the Finite Difference Method [17,18] and the Boundary Element Method [19-21] are available, yet the most

popular and commonly used method for the solution of time-dependent inelastic problems remains the Finite Element Method, or FEM [5,6,12, 15,22-25].

Since, as already pointed, the differential equations associated with these models are "stiff" in nature, these present a great deal of difficulty for a time-dependent analysis. It is, therefore, necessary that suitable integration algorithms - fast, stable and economic (in computer time) - be developed for viscoplastic models so that these models could be used conveniently on a practical scale and lead to a more realistic and rational design of structural components for use at elevated temperatures. The important and basic criterion in the development of any integration algorithm for the stiff equations of the viscoplastic models is that it must be usable with the Finite Element Method (or the Finite Difference or Boundary Element Methods). It is with this objective of developing a fast, stable and economic numerical integration strategy (to be used in conjunction with the Finite Element Method) for viscoplastic models that the work presented in this report was carried out. Out of a number of viscoplastic models now available in literature, the more commonly used models due to Bodner-Partom [1-2], Robinson [4] and Walker [6] were selected for the development and assessment of the integration algorithms. These models have different mathematical structures. For example, the Robinson model utilizes the concept of a yield surface together with the loading and unloading criteria, whereas the other two do not. A detailed review of these models and their capabilities may be found in Ref.[23]. The uniaxial forms of these models for isothermal conditions are presented in the following section.

## 2. Viscoplastic Models (Uniaxial Forms)

### 2.1 Bodner-Partom Model

The uniaxial form of the equations for Bodner-Partom model is:

$$\dot{\epsilon} = \dot{\epsilon}_e + \dot{\epsilon}_I \quad , \quad (1)$$

$$\dot{\epsilon}_e = \dot{\sigma}/E \quad , \quad (2)$$

$$\dot{\epsilon}_I = \frac{2}{\sqrt{3}} D_0 \frac{\sigma}{|\sigma|} \exp \left[ - \left( \frac{n+1}{2n} \right) \left( \frac{Z^2}{\sigma^2} \right)^n \right] \quad , \quad (3)$$

$$\dot{Z} = m (Z_1 - Z) \dot{W}_p - A Z_1 \left( \frac{Z - Z_I}{Z_1} \right)^r \quad , \quad (4)$$

and

$$\dot{W}_p = \sigma \dot{\epsilon}_I \quad . \quad (5)$$

In which  $\epsilon$  is the strain and  $\sigma$  the stress. The subscripts 'e' and 'I' refer to elastic and inelastic components and the dot over a symbol denotes differentiation with respect to time  $t$ . The quantities  $E$ ,  $D_0$ ,  $n$ ,  $m$ ,  $Z$ ,  $A$ ,  $Z_1$  and  $r$  are material constants and listed in Table-I(a). The variable  $Z$  is a measure of isotropic hardening or dislocation density and is called the 'drag' stress.  $\dot{W}_p$  is the rate of plastic work. The first term in eq.(4) represents work hardening and the second term (through the constants  $A$ ,  $r$  and  $Z_1$ ), allows for thermal recovery or softening.

## 2.2 Robinson Model

The nondimensional uniaxial form of Robinson model for the case of pure shear may be written as:

$$B\tau' = \begin{cases} F^{\frac{n-1}{2}} (\tau - \alpha) & ; \begin{cases} F > 0, \tau \alpha > 0 \text{ and } \tau(\tau - \alpha) > 0, \\ F > 0 \text{ and } \tau \alpha \leq 0. \end{cases} \\ 0 & ; \begin{cases} F \leq 0, \\ F > 0, \tau \alpha > 0 \text{ and } \tau(\tau - \alpha) \leq 0 \end{cases} \end{cases} \quad (6)$$

$$\dot{\alpha}' = \begin{cases} \frac{B\tau'}{|\alpha|^\beta} - R\alpha|\alpha|^{n-\beta-1} & ; |\alpha| > \alpha_0 \text{ and } \tau\alpha > 0, \\ \frac{B\tau'}{|\alpha_0|^\beta} - R\alpha\alpha_0^{n-\beta-1} & ; |\alpha| \leq \alpha_0 \text{ or } \tau\alpha \leq 0; \end{cases} \quad (7)$$

where

$$F = (\tau - \alpha)^2 - 1, \quad \alpha_0 = G_0^{1/2} > 0.$$

Equations (6) are referred to as flow laws and eqs.(7) as evolution laws.  $\alpha$  is the nondimensional back stress,  $\tau$  - the nondimensional applied shear stress, and  $\gamma$  - the inelastic shear strain. The evolution law includes two terms - one corresponding to a hardening process and the other to softening or recovery of the material and is based on the Bailey-Orowan theory [26].  $B$ ,  $n$ ,  $R$ ,  $\beta$ ,  $G_0$  are material parameters and prime (') denotes differentiation with respect to nondimensional time  $T$  (cf.Ref.[4]). The material constants for Robinson model are given in Table I(b).

### 2.3 Walker Model

The equations for the uniaxial case of Walker model have the following form:

$$\dot{\epsilon}_I = K^{-n} |\sigma - \Omega|^{n-1} |\sigma - \Omega|, \quad (8)$$

$$\dot{\Omega} = (n_1 + n_2) \dot{\epsilon}_I - (\Omega - n_1 \epsilon_I) \dot{G}, \quad (9)$$

$$\dot{G} = (n_3 + n_4 e^{-n_5 R}) \dot{R} + n_6 |\Omega|^{m-1}, \quad (10)$$

$$\dot{R} = |\dot{\epsilon}_I|, \quad (11)$$

$$K = K_1 - K_2 e^{-n_7 R}, \quad (12)$$

and

$$\sigma = E(\epsilon - \epsilon_I) \quad (13)$$

The quantities  $K_1$ ,  $K_2$ ,  $n$ ,  $n_1$ ,  $n_2$ ,  $n_3$ ,  $n_4$ ,  $n_5$ ,  $n_6$ ,  $n_7$  and  $m$  are material constants listed in Table- I(c).  $\Omega$  is the back stress and accounts for the Bauschinger effect or kinematic hardening. The first term in eq.(10) corresponds to the dynamic strain recovery, whereas the second term to the static thermal recovery for the back stress.  $K$  is called the drag stress variable.

### 3. Numerical Integration Methods

Stiff Equations: A system of differential equations, in which a small change in the values of independent variables may cause a large change in the values of dependent variables is called a "stiff" system of equations. A more rigorous definition of 'stiffness' may be found in Ref.[27].

Since the differential equations associated with the viscoplastic models and governing the growth of internal state variables are stiff equations, special care and attention is called for their integration. For use in conjunction with a finite element code, these equations are to be integrated a large number of times. The cost and computer time involved, therefore, prohibit the use of traditional methods of using small time steps for accurate integration of these stiff equations. A 'smart' integration strategy with automatic time-step control capable of achieving the desired accuracy and stability is, therefore, required. This integration strategy, together with one of the single or multistep, implicit or explicit numerical methods reported in literature [27,28] may then be implemented into a finite element code for optimal results. Kumar et al.\* [29] present several

---

\*Several other attempts to integrate these stiff equations have been made and some useful information in this regard is available in literature [30-32].

such integration strategies and show that in case of inelastic model due to Hart [7], the use of a simple one step explicit Euler integration scheme with automatic time-step control is advantageous.

Another favourable aspect of the explicit integration schemes over the implicit integration schemes is that they do not require the evaluation or inversion of a Jacobian matrix. This fact is of advantage and significance especially when the number of equations involved is large. The advantage of using implicit integration methods is that they may allow large time steps without affecting the stability of the method. Cormeau [33] has, however, shown that several implicit methods suffer from the same time-step restriction as does the Euler method and in such circumstances the implicit methods offer no special advantages over the simpler explicit methods.

With these considerations in mind, the following explicit integration methods were selected for further investigations:

1. Euler method,
2. Modified Euler method,
3. Fourth Order Runge-Kutta method, and
4. Milne's predictor-corrector method.

The formulae for these methods in case of a system of equations are given in Table II. The first three of these methods are single step methods whereas the fourth - Milne's method - is a multistep method. During the course of numerical computations, it was observed that smaller time-step sizes than those required for Euler, Modified Euler and Runge-Kutta method were required for the stability of Milne's method. Further, being a multistep method the requirement of a large storage space (when used for integration with a finite element programme) discourages the use of Milne's method. These considerations resulted in the exclusion of Milne's method from further investigations.

### 3.1 Comparison of the Integration Methods

Because of highly non-linear and stiff character of differential equations associated with the three viscoplastic models due to

Bodner-Partom, Robinson and Walker, it is natural to expect that the integration of equations may be sensitive to the integration method being used. (It will, of course, also depend on the particular viscoplastic model being integrated). To explore this further, a considerable amount of computations\* was carried out for the three viscoplastic models using the above mentioned integration methods and different (constant) time steps. Some of the results of these computations are listed in Tables III(a), III(b), III(c) and Figures 2 through 4, for Bodner- Partom, Robinson and Walker models, respectively. The cyclic loadings used with these models are shown in Figure 1 and are taken from References [34], [4] and [6], respectively.

The values of stress for Bodner-Partom model at different times, obtained using the three integration methods, for a number of time-step sizes were calculated and the values for time step sizes,  $\Delta t = 0.5, 0.005$  and  $0.001$  are shown in Table III(a). It is found that for these time step sizes, the differences in the values of stress for the three integration methods is negligibly small. (These differences may be large if a sufficiently large time step is taken). And, as expected, with the reduction of time step size, the values obtained using different integration methods get improved. It is also seen that to obtain the 'accurate' values (defined as the values which change insignificantly with further reduction of time step size) of stress, the same small time-step has to be used for all the three integration methods. The CPU-times for these three methods for any time-step size are, however, strikingly different.

For example, for  $\Delta t = 0.005$  and  $\Delta t = 0.001$ , the CPU-times for Euler, Modified Euler and Runge-Kutta methods are, respectively: 0.84, 3.78, 3.20; and 3.99, 18.85, 15.39 seconds (and the number of iterations per cycle are 20,000; and 100,000 respectively). It may, therefore, be noted that the CPU-time required for the Euler method is significantly less than that required for the other two methods.

---

\* All the computations presented in this report were performed on a SIEMENS M7890 machine. The double precision arithmetic was used to reduce the errors due to truncation.

Table III(b) depicts the values of non-dimensional stress for Robinson model, obtained using the three integration methods. The time step sizes are  $\Delta t = 0.2 \times 10^{-5}$ ,  $0.1 \times 10^{-5}$  and  $0.5 \times 10^{-6}$ . Similar results as those mentioned in the preceding paragraph for Bodner-Partom model seem to hold good for this model, too. The CPU-times required for the Euler, Modified Euler and Runge-Kutta methods for the aforementioned time-step sizes are: 0.78, 3.52, 2.86, 1.51, 6.96, 5.64; and 2.87, 13.69, 11.15 seconds, respectively (and the number of iterations per cycle is 10,000; 20,000; and 40,000; respectively). The Euler method is found to be the most economic (in computer time) method for this model, too.

The values of stress in case of Walker model for  $\Delta t = 0.0025$ ,  $0.001$  and  $0.00025$  are exhibited in Table III(c), for the three integration methods. It is seen that for  $\Delta t = 0.0025$  the difference in the values of stress obtained using the Euler method and those obtained using the Modified Euler and Runge-Kutta methods is quite apparent. But this difference decreases with the reduction in time-step size to obtain the accurate values. For example, for  $\Delta t = 0.00025$  the differences in the values predicted by the three methods are negligibly small. The CPU-times required for the Euler, Modified Euler and Runge-Kutta methods for time steps,  $\Delta t = 0.0025$ ,  $\Delta t = 0.001$  and  $\Delta t = 0.00025$  are, respectively, 0.47, 1.49, 1.24; 0.85, 3.38, 12.78 and 2.79, 12.50 and 10.47 seconds (and the number of iterations per cycle is 2,480; 6200; and 24,800; respectively). The Euler method is again seen to consume the minimum computer time to yield the accurate values of stress in case of Walker model, too.

The foregoing results and observations suggest that the use of Euler method with an automatic time-step integration strategy should lead to an optimal integration algorithm for the integration of stiff constitutive equations associated with these models, and for incorporation into a Finite Element Code (like ABAQUS, ADINA or MARC, etc.) Naturally, the next step, therefore, was to develop or to use already existing automatic time-step control strategies in conjunction

with the Euler method and assess their capabilities with regard to the viscoplastic models mentioned herein. The integration strategies examined during the course of present work are outlined in the next section.

#### 4. Integration Strategies With Automatic Time-Step Control

There are different integration strategies that have been proposed or successfully used by various investigators [6,29-31,35] for viscoplastic and creep problems. Some of these, and the integration strategy developed during the course of present investigations, are listed below:

##### 4.1 Automatic Time-Step Control Integration Strategies Based On Taylor's Expansion

Expanding the strain  $\epsilon$  at any time  $t+\Delta t$  by Taylor's series, we have

$$\epsilon(t + \Delta t) = \epsilon(t) + \Delta t \dot{\epsilon} + \frac{(\Delta t)^2}{2!} \ddot{\epsilon} + \dots \quad (14)$$

The time step  $\Delta t$  is then chosen so that the second term in the series is some small fraction, say  $\lambda$ , of the first term. This yields

$$\Delta t = \lambda \frac{|\epsilon|}{|\dot{\epsilon}|} \quad (15)$$

Such a time increment has been used for the solution of creep problems [35].

If the time step  $\Delta t$  is so chosen that the third term in expansion (14) is some small fraction, say  $\mu$ , of the second term, one obtains

$$\Delta t = 2\mu \frac{|\dot{\epsilon}|}{|\ddot{\epsilon}|} \quad (16)$$

Such a choice of time step has been suggested by Lindholm et al. [23] for viscoplastic problems.

The Euler method with automatic time step increments, as suggested in eq.(15) or eq.(16), was used for integrating the constitutive equations associated with the Bodner-Partom, Robinson and Walker models. The integration strategies worked well in the initial stages of computations but later allowed time steps large enough to cause instability. It was observed during the calculations that choosing small values for  $\lambda$  and  $\mu$  delayed the onset of instability but it could not be completely avoided. These two integration strategies were, therefore, not further explored.

#### 4.2 Integration Strategy Proposed By Kumar et al.

Kumar et al. [29], have proposed and employed an automatic time-step integration strategy with explicit Euler method for the integration of inelastic constitutive equations due to Hart [7]. The strategy was found to be promising upon its comparison with several other integration strategies reported therein. A brief outline of the strategy proposed by them is given below.

For the single differential equation

$$\frac{dy}{dt} = \phi(y, t) \quad , \quad (17)$$

the value of  $y$  at  $t+\Delta t$  can be obtained as

$$y(t + \Delta t) = y(t) + \Delta t \phi(y, t) \quad . \quad (18)$$

The error,  $e$ , at this step and used for time step control is then defined as

$$e = \Delta t \left| \nabla \phi / y(t) \right| \quad , \quad (19)$$

where  $\nabla\phi$  is the first backward difference of  $\phi$ .

Two error parameters  $e_{\max}$  and  $e_{\min}$  are prescribed. The strategy works as follows:

Compute  $e$ , if  $e_{\max} < e$  : replace  $\Delta t$  by  $\Delta t/2$ , recompute  $e$ ,  
 $e \leq e_{\max}$  : accept  $\Delta t$ ; compute  $y(t + \Delta t)$ .

The time step for the next step,  $\Delta t_{\text{new}}$ , is defined as follows:

if  $e_{\min} < e \leq e_{\max}$  :  $\Delta t_{\text{new}} = \Delta t$ ,  
 and  
 if  $e \leq e_{\min}$  :  $\Delta t_{\text{new}} = 2 \Delta t$ .

It is easy to extend the method for a system of differential equations

$$\frac{dy^{(i)}}{dt} = \phi^{(i)}(y^{(i)}, t), \quad (20)$$

by defining an error vector  $e^{(i)}$ , as before.

Now a suitable norm

$$e = L^n(e^{(i)}), \quad (21)$$

is defined. Three common norms suggested by Kumar et al. and used in the present work are

$$\begin{aligned} L^\infty &= \max |e^{(i)}|, \\ L^1 &= \sum_i |e^{(i)}|, \quad \text{and} \\ L^2 &= \sqrt{\sum [e^{(i)}]^2}. \end{aligned} \quad (22)$$

The values of stress for respective cyclic loadings, as depicted in Fig.1, for Bodner-Partom model (one cycle), Robinson model (two and one-quarter of a cycle) and Walker model (two and one-quarter of a cycle) have been calculated using the abovementioned algorithm and for the three error norms mentioned in eq.(22). Since the values obtained using the three norms differed negligibly, the values only for the norm,  $L^\infty$ , are tabulated in Tables IV(a), IV(b) and IV(c) for the three viscoplastic models. The values have been listed for twenty points per complete cycle (ten for loading and ten for unloading). The third and sixth columns of these Tables show the corresponding 'accurate' values obtained using a constant time step (cf. Section 3.1). Figures 2-4 show the accurate values for one cycle for Bodner-Partom model and one and one-quarter of a cycle for Robinson and Walker models. The solid circles (triangles) show the points taken on the cycles for comparing the stress values due to Kumar et al. (present) integration strategy with the accurate stress values.

#### 4.3 Present Integration Strategy

The integration strategy developed during the course of present investigations will now be illustrated for the differential equation:

$$\frac{dy}{dt} = \phi(y, t) \quad (17)$$

Suppose that the solution of eq.(17) at any time  $t$  is known or obtainable using any one of the integration methods. To obtain the solution at the next time step, the integration strategy proceeds as follows:

I. Choose a suitable time step,  $\Delta t$ , say. Denote the value of  $y$  obtained with this time step as  $Y_F(=y_{t+\Delta t})$ .

II. Halve the time step  $\Delta t$ . Denote the value of  $y$  obtained

(in two steps) as  $Y_H (= y_{t+\Delta t})$ .

III. Define the quantity

$$\text{Tol} = \frac{|Y_F - Y_H|}{|Y_H|} \quad (23)$$

The upper and lower limits for the quantity Tol (say, tolerance) are prescribed and denoted as  $\text{Tol}_u$  and  $\text{Tol}_l$ , respectively. The next steps in the strategy are:

IV. If  $\text{Tol} > \text{Tol}_u$ , replace  $\Delta t$  by  $\Delta t/2$ . Go to step I. Re-compute Tol by repeating steps I through III. Repeat the procedure until a time step  $\Delta t$  is obtained for which  $\text{Tol} \leq \text{Tol}_u$ . Accept the corresponding value of  $y$  as the value  $y_{t+\Delta t}$ .

V. Compare Tol with  $\text{Tol}_l$ . If  $\text{Tol}_l \geq \text{Tol}$ , double the time step as used in step IV for the next step calculations. And, if  $\text{Tol}_l < \text{Tol}$ , retain the time step used in step IV for next step calculations.

VI. Repeat the procedure with the time step rendered by step V, and so on.

The strategy can easily be generalized to a system of equations by using concepts similar to those mentioned in Section 4.2.

The values of stresses obtained for Bodner-Partom, Robinson and Walker models in case of respective loadings (cyclic) have been tabulated in column 5 of Tables IV(a) through IV(c), respectively. The corresponding 'accurate' values have been shown in column 6 of these Tables. Another important point that is brought forward from these Tables is the fact that these integration strategies admit maximum error in the regions where the stress changes from tensile to compressive and vice versa.

## 5. Discussions

In order to analyse the capabilities and efficiency of the integration strategies with automatic time step control presented in Sections 4.2 and 4.3, the following error norm was defined:

$$\xi = \left[ \sum \left( \frac{\sigma - \sigma_a}{\sigma_a} \right)^2 \right]^{1/2} \quad (24)$$

where  $\sigma$  denotes the value of stress obtained using the integration strategy (Kumar et al. or present) and  $\sigma_a$  denotes the corresponding 'accurate' value of stress taken from Column 3 or Column 6 of Tables IV.

### 5.1 Bodner-Partom Model

The values of stress at different times obtained by using the two integration strategies and for the cyclic loading shown in Fig.1(a), have been listed in Columns 2 and 5 of Table IV(a). Columns 3 and 6 of this table show the corresponding accurate values. The error norms, as defined in eq.(24), have been calculated by taking twenty points per complete cycle (at equal spaces wherever possible) for Kumar et al. and present integration strategies and denoted by  $\xi_K$  and  $\xi_P$ , respectively. The error norms at the peak values of stress during loading or unloading were also calculated and denoted by  $\xi_{KP}$  and  $\xi_{PP}$ , respectively, for the two integration strategies. The values of all the error norms and CPU-times (on a SIEMENS M7890 machines) in case of Bodner-Partom model are reproduced from Table V and listed below:

Kumar et al. Strategy

$$\xi_K = 0.1887,$$

$$\xi_{KP} = 3 \times 10^{-7},$$

CPU-Time = 0.55 secs.

Present Strategy

$$\xi_P = 0.00225,$$

$$\xi_{PP} = 2 \times 10^{-8},$$

CPU-Time = 0.16 secs.

The Table IV(a) also shows the values of  $e_{\min}$  ( $=10^{-4}$ ) and  $e_{\max}$  ( $=10^{-3}$ ) and of  $Tol_l$  ( $=10^{-5}$ ) and  $Tol_u$  ( $=10^{-4}$ ), used for the two integration strategies.\* It is seen that the present integration strategy not only works faster than the strategy proposed by Kumar et al. but also yields more accurate results in case of Bodner-Partom model.

## 5.2 Robinson Model

The values of nondimensional shear stress for nondimensional times (shear strains) have been listed for Robinson model for the two integration strategies in Table IV(b). The loading cycle is shown in Fig.1(b). The results listed are for two and one-quarter of a cycle of this loading and are obtained including the elastic components.

The values of error norms and CPU-times reproduced from Table V are:

Kumar et al. Strategy	Present Strategy
$\xi_K = 0.0543$	$\xi_P = 0.0045$ ,
$\xi_{KP} = 2 \times 10^{-6}$	$\xi_{PP} = 5 \times 10^{-7}$ ,
CPU-Time = 0.63 secs.	CPU-Time = 0.48 secs.

The integration strategy presented in this report is seen to work more efficiently and accurately than that proposed by Kumar et al. for Robinson model also.

---

\* In fact the values of  $e_{\min}$ ,  $e_{\max}$ ,  $Tol_l$  and  $Tol_u$  were at first selected arbitrarily and reduced further until results close to the accurate values of stress were obtained. The values listed in this and other Tables are these values of error norms and tolerances.

### 5.3 Walker Model

Table IV(c) exhibits the values of stresses obtained at different times (strains) for the loading cycle (two and one-quarter of a cycle) shown in Fig.1(c) for the two strategies. The values of error norms and CPU-times for these are shown below:

Kumar et al. Strategy	Present Strategy
$\xi_K = 0.0498$	$\xi_P = 0.4517,$
$\xi_{KP} = 1 \times 10^{-6}$	$\xi_{PP} = 0.67 \times 10^{-5},$
CPU-Time = 0.51 secs.	CPU-Time = 0.76 secs.

It is seen, therefore, that the present strategy does not work as well for Walker model as it did in case of Bodner-Partom and Robinson models. In fact, the strategy due to Kumar et al. works faster and yields more accurate results. This observation, therefore, supports the apprehension that the success of an integration strategy also depends on the viscoplastic model being integrated. It also serves as a warning that, in order to obtain optimum results, an integration strategy with automatic time control should be used with care. Table V gives a general overview of how the two integration strategies work in case of different viscoplastic models. The informations furnished therein may possibly be exploited beneficially by a structural analyst.

### 6. Conclusions

The report deals with the problem of numerical integration of non-linear and stiff differential equations associated with the unified viscoplastic models. Some integration methods have been examined in detail and, on the basis of a large amount of computations carried out during the course of present work, the use of a simple explicit Euler method with an automatic time step control is seen to be most encouraging. Several automatic time step control strategies have been presented and discussed to assess their applicability in con-

junction with a Finite Element Programme. The capabilities of automatic time integration strategies - one proposed by Kumar et al. and the other presented in the report - are estimated in case of viscoplastic models due to Bodner-Partom, Robinson and Walker (uniaxial forms). It is concluded that the success of an automatic time step integration strategy is linked with the model being integrated. It is expected that the results presented in the report may be of help and provide some useful guidelines to analysts and engineers for integrating the stiff constitutive equations of viscoplastic models.

#### Acknowledgements

The author (VKA) wishes to place on record his indebtedness to Professor-Dr. D. Munz, Director, IMF IV, Kernforschungszentrum Karlsruhe, for providing an invaluable opportunity to work on this problem.

REFERENCES

1. Bodner, S.R. and Y.Partom: Constitutive Equations for Elastic-Viscoplastic Strain Hardening Materials. ASME Journal of Applied Mechanics. 42, 385-389, 1979.
2. Bodner, S.R.: Representation of Time Dependent Mechanical Properties of Rene 95 by Constitutive Equations. Air Force Materials Laboratory. AFML-TX-79-4116, 1979.
3. Merzer, A. and S.R. Bodner: Analytical Formulation of a Rate and Temperature Dependent Stress-Strain Relation. Journal of Engineering Materials and Technology. 101, 254-257, 1979.
4. Robinson, D.N.: A Unified Creep-Plasticity Model For Structural Metals at High Temperatures. Oak Ridge National Laboratory - ORNL/TM-5969, 1978.
5. Robinson, D.N. and R.W. Swindeman: Unified Creep-Plasticity Constitutive Equations for 2-1/4 Cr-1 Mo Steel at Elevated Temperature. Oak Ridge National Laboratory - ORNL/TM-8444, 1982.
6. Walker, K.P.: Research and Development Program for Non-Linear Structural Modeling with Advanced Time-Temperature Dependent Constitutive Relationships. NASA CR-165533, 1981.
7. Hart, E.W.: Constitutive Relations for the Nonelastic Deformation of Metals. ASME Journal of Engineering Materials and Technology. 98, 193-202, 1976.
8. Valanis, K.C.: Constitutive Equations in Viscoplasticity. Phenomenological and Physical Aspects. ASME-AMD, Vol.21, 1976.

9. Chaboche, J.L.: Viscoplastic Constitutive Equations for the Description of Cyclic and Anisotropic Behavior of Metals. Bulletin de L'Academie des Sciences, Series des Sciences Techniques. XXV, 33-42, 1977.
10. Miller, A.K.: Development of the Materials Code, MATMOD Constitutive Equations for Zircaloy. EPRI Report No. EPRI-NP-567, December 1977.
11. Kagawa, H. and Y. Asada: Extension of Miller's Constitutive Model for Multiaxial Deformation. Proceedings of ASME International Conference on Advances in Life Prediction Methods, Albany, New York, pp.33-39, 1983.
12. Walker, K.P.: Constitutive Modeling of Engine Materials. Final Report FR-17911 to AFML, Nov.1983.
13. Krieg, R.D., J.C. Swearngen and R.W. Rohde: A Physically Based Internal Variable Model for Rate-Dependent Plasticity. In Inelastic Behavior of Pressure Vessel and Piping Components. PVP-PB-028 (ASME), pp.15-28, 1978.
14. Cernocky, E.P. and E. Krempl: A Nonlinear Uniaxial Integral Constitutive Equation Incorporating Rate Effects, Creep and Relaxation. International Journal of Nonlinear Mechanics. 14, 183-203, 1979.
15. Zienkiewicz, O.C. and Corneau, I.C.: Visco-Plasticity, Plasticity and Creep in Elastic Solids - A Unified Numerical Approach. International Journal for Numerical Methods in Engineering. 8, 821-845, 1974.
16. Bruhns, O.T., B. Boecke, F. Link: The Constitutive Relations of Elastic-Inelastic Materials at Small Strains. Nuclear Engineering and Design. 83, 325-331, 1984.

17. Mukherjee, S., V. Kumar and K.J. Chang: Elevated Temperature Inelastic Analysis of Metallic Media Under Time-Varying Loads Using State Variable Theories. International Journal of Solids and Structures. 14, 663-679, 1978.
18. Chang, K.J., R.H. Lance and S. Mukherjee: Inelastic Bending of Beams Under Time-Varying Moments - A State Variable Approach. Third National Pressure Vessels and Piping Congress of the ASME, San Francisco, California, 1979.
19. Kumar, V. and S. Mukherjee: A Boundary Integral Equation Formulation for Time-Dependent Inelastic Deformation in Metals. International Journal of Mechanical Sciences. 19, 713-724, 1977.
20. Mukherjee, S. and V. Kumar: Numerical Analysis of Time-Dependent Inelastic Deformation in Metallic Media Using the Boundary-Integral Equation Method. ASME Journal of Applied Mechanics. 45, 785-790, 1978.
21. S. Mukherjee: Boundary Element Methods in Creep and Fracture. Applied Science Publishers, London, 1982.
22. Kumar, V., F. Huang, S. Mukherjee and C.Y. Li: Theoretical and Experimental Analysis of Stresses in Reactor Components: Deformation in Type 304 Stainless Steel. EPRI Final Report for Contract No. RP 697-1, Department of Materials Science and Engineering, Cornell University, Ithaca, NY, USA, 1979.
23. Lindholm, U.S., K.S. Chan, S.R. Bodner, R.M. Weber, K.P. Walker, B.N. Cassenti: Constitutive Modeling for Isotropic Materials (HOST). NASA CR-174718, 1984.

24. Kaufman, A., J.H. Laflen and U.S. Lindholm: Unified Constitutive Material Models for Non-Linear Finite Element Structural Analysis. NASA Technical Memorandum No. 86985, 1985.
25. Cassenti, B.N.: Research and Development Program for the Development of Advanced Time Temperature Dependent Constitutive Relationships. NASA CR-168191, 1983.
26. Orowan, E.: The Creep of Metals. J.W. Scotl. Iron Steel Institute. 54, 45-53, 1946.
27. Lambert, J.D.: Computational Methods in Ordinary Differential Equations. Wiley, London, 1973.
28. Roberts, C.E. (Jr.): Ordinary Differential Equations - A Computational Approach. Prentice-Hall, 1979.
29. Kumar, V., M. Morjaria and S. Mukherjee: Numerical Integration of Some Stiff Constitutive Models of Inelastic Deformation. ASME Journal of Engineering Materials and Technology. 102, 92-96, 1980.
30. Krieg, R.D.: Numerical Integration of Some New Unified Plasticity-Creep Formulations. Transactions of the 4th International Conference on Structural Mechanics in Reactor Technology, San Francisco, USA, 1977. Paper No. M6/4.
31. Chang, T.Y., J.P. Chang and R.L. Thompson: On Numerical Integration and Computer Implementation of Viscoplastic Models (unpublished).
32. Haisler, W.E. and P.K. Imbrie: Numerical Considerations in the Development and Implementation of Constitutive Models (unpublished).

33. Cormeau, I.: Numerical Stability in Quasi-Static Elasto/ Visco-Plasticity. International Journal for Numerical Methods in Engineering. 9, 109-127, 1975.
34. Milly, T.M and D.H. Allen: A Comparative Study of Nonlinear Rate-Dependent Mechanical Constitutive Theories for Crystalline Solids at Elevated Temperatures. Report No. VPI-E-82-5, Virginia Polytechnic Institute and State University, Blacksburg, Virginia, USA, 1982.
35. Penny, R.K. and D.L. Mariott: Design for Creep. Mc Graw Hill, 1971.
36. Stouffer, D.C.: A Constitutive Representation for IN100. Air Force Materials Laboratory-Report No. AFWAL-TR-80-4180, 1980.

Table - I(a)

Material Constants\* for Bodner-Partom Model

$E = 21.3 \times 10^3$ KSI	$D_o = 10^4 \text{ sec}^{-1}$
$n = 0.7$	$A = 1.9 \times 10^{-3} \text{ sec}^{-1}$
$Z_1 = 1015$ KSI	$r = 2.66$
$Z_o = 915$ KSI	$Z_I = 600$ KSI
$m = 2.57$ KSI <sup>-1</sup>	

\*These constants taken from Ref. (36) are for IN100 at 1350°F.

Table - I(b)

Material Constants\* for Robinson Model

$B = 3000$	$\beta = 1$
$R = 0.1$	$\alpha_o = 0.001$
$n = 4$	$g = 10.000$

\*Taken from Ref. (4).

Table I(c)

Material Constants\* for Walker Model

$\lambda = 11.5 \times 10^6$	$n_2 = 1 \times 10^6$
$\mu = 4.9 \times 10^{-6}$	$n_3 = 312$
$K = 59292$	$n_4 = 0$
$K_2 = 0$	$n_5 = 0$
$n = 4.49$	$n_6 = 2.73 \times 10^{-3}$
$m = 1.16$	$n_7 = 0$
$n_1 = 0$	$\Omega^o = -1200$

\*\*These constants taken from Ref. (6), are for Hastelloy-X at 1800°F.

Table - II

Formulae For Numerical Integration Methods

Consider the vector initial value problem

$$\frac{d\tilde{Y}}{dx} = \tilde{f}(x, \tilde{Y}), \quad \tilde{Y}(x_0) = \tilde{C}_0 \quad (1)$$

Let  $x_n = x_0 + nh$  and  $\tilde{Y}_n = \tilde{Y}(x_n)$  and let  $\tilde{f}_n = \tilde{f}(x_n, \tilde{Y}_n)$ .

The integration formulae are:

I. Euler Method:

$$\tilde{Y}_{n+1} = \tilde{Y}_n + h\tilde{f}_n .$$

II. Modified Euler Method:

$$\begin{aligned} \tilde{Y}_{n+1}^P &= \tilde{Y}_n + h\tilde{f}_n \\ \tilde{Y}_{n+1}^C &= \tilde{Y}_n + \frac{h}{2} \{ \tilde{f}_n(x_n, \tilde{Y}_n) + \tilde{f}_n(x_{n+1}, \tilde{Y}_{n+1}^P) \}, \\ \tilde{Y}_{n+1}^{new} &= \tilde{Y}_n + \frac{h}{2} \{ \tilde{f}_n(x_n, \tilde{Y}_n) + \tilde{f}_n(x_{n+1}, \tilde{Y}_{n+1}^{C*}) \}. \end{aligned} \quad (2)$$

(\*In this term the latest available values of different components of  $\tilde{Y}_{n+1}^C$  are used.)

III. Fourth Order Runge-Kutta Method:

$$\tilde{Y}_{n+1} = \tilde{Y}_n + \frac{h(k_1 + 2k_2 + 2k_3 + k_4)}{6}, \quad (3)$$

where

$$\begin{aligned} k_1 &= \tilde{f}_n = \tilde{f}(x_n, \tilde{Y}_n), \\ k_2 &= \tilde{f}(x_n + \frac{h}{2}, \tilde{Y}_n + \frac{h}{2}k_1), \\ k_3 &= \tilde{f}(x_n + \frac{h}{2}, \tilde{Y}_n + \frac{h}{2}k_2), \\ k_4 &= \tilde{f}(x_{n+h}, \tilde{Y}_n + hk_3). \end{aligned} \quad (4)$$

IV. Milne's Predictor-Corrector Method:

Predictor

$$y_{n+1}^p = y_{n-3} + \frac{4h(2 f_{\tilde{n}} - f_{\tilde{n}-1} + 2 f_{\tilde{n}-2})}{3}, \quad (5)$$

Corrector

$$y_{n+1}^j = y_{n-1} + \frac{h(f(x_{n+1}, y_{n+1}^{k-1}) + 4 f_{\tilde{n}} + f_{\tilde{n}-1})}{3}, \quad (6)$$

$$j = 1, 2, \dots$$



Table III(b)

Values of nondimensional stress vs nondimensional time (strain) for Robinson Model.

Stress Time	$\Delta t = 0.2 \times 10^{-5}$			$\Delta t = 0.1 \times 10^{-5}$			$\Delta t = 0.5 \times 10^{-6}$		
	Euler	M.Euler	Runge	Euler	M.Euler	Runge	Euler	M.Euler	Runge
0.0025 (0.0025)	10.242	10.242	10.242	10.241	10.241	10.241	10.241	10.241	10.241
0.0050 (0.0050)	12.095	12.094	12.094	12.094	12.094	12.094	12.094	12.094	12.094
0.0075 (0.0025)	-8.808	-8.808	-8.808	-8.807	-8.807	-8.807	-8.806	-8.806	-8.806
0.0100 (0.0)	-11.369	-11.369	-11.369	-11.369	-11.368	-11.368	-11.368	-11.368	-11.368
0.0125 (-0.0025)	-12.855	-12.855	-12.855	-12.854	-12.854	-12.854	-12.854	-12.854	-12.854
0.0150 (-0.0050)	-13.998	-13.997	-13.997	-13.997	-13.997	-13.997	-13.997	-13.997	-13.997
0.0175 (-0.0025)	8.403	8.403	8.403	8.401	8.401	8.401	8.400	8.400	8.400
0.0200 (0.0)	11.234	11.234	11.234	11.233	11.233	11.233	11.233	11.233	11.233
0.0225 (0.0025)	12.758	12.757	12.757	12.757	12.757	12.757	12.757	12.757	12.757
0.0250 (0.0050)	13.919	13.919	13.919	13.919	13.919	13.919	13.919	13.918	13.918
0.0275 (0.0025)	-8.422	-8.422	-8.422	-8.420	-8.420	-8.420	-8.419	-8.419	-8.419
0.0300 (0.0)	-11.240	-11.239	-11.239	-11.239	-11.239	-11.239	-11.239	-11.239	-11.239
0.0325 (-0.0025)	-12.762	-12.761	-12.761	-12.761	-12.761	-12.761	-12.761	-12.761	-12.761
0.0350 (-0.0050)	-13.923	-13.922	-13.922	-13.922	-13.922	-13.922	-13.922	-13.922	-13.922
0.0375 (-0.0025)	8.421	8.421	8.421	8.419	8.419	8.419	8.418	8.418	8.418
0.0400 (0.0)	11.240	11.239	11.239	11.239	11.239	11.239	11.238	11.238	11.238
0.0425 (0.0025)	12.762	12.761	12.761	12.761	12.761	12.761	12.761	12.761	12.761
0.0450 (0.0050)	13.923	13.922	13.922	13.922	13.922	13.922	13.922	13.922	13.922

Table III(c)

Values of stress (psi) at different times (strains) for Walker Model .

Stress (psi) Time (strain)	$\Delta t = 0.0025$			$\Delta t = 0.001$			$\Delta t = 0.00025$		
	Euler	Modified Euler	Runge Kutta	Euler	Modified Euler	Runge Kutta	Euler	Modified Euler	Runge Kutta
0.31 (0.0012)	13808	13820	13820	13795	13800	13800	13789	13790	13790
0.62 (0.0024)	16700	16772	16772	16710	16724	16724	16711	16718	16718
0.93 (0.0036)	17457	17546	17547	17479	17497	17497	17482	17491	17491
1.24 (0.0048)	17973	18068	18069	18000	18019	18019	18003	18012	18013
1.55 (0.0060)	18339	18434	18434	18365	18384	18384	18368	18378	18378
1.86 (0.0048)	373	448	449	419	449	449	441	449	449
2.17 (0.0036)	-13633	-13590	-13589	-13588	-13571	-13571	-13566	-13562	-13562
2.48 (0.0024)	-17156	-17204	-17204	-17150	-17170	-17170	-17148	-17153	-17153
2.79 (0.0012)	-18443	-18527	-18527	-18457	-18491	-18491	-18465	-18473	-18473
3.10 (0.0)	-19358	-19459	-19459	-19382	-19423	-19423	-19394	-19404	-19404
3.41 (-0.0012)	-20016	-20123	-20123	-20043	-20086	-20086	-20057	-20067	-20068
3.72 (-0.0024)	-20485	-20591	-20592	-20511	-20554	-20554	-20525	-20535	-20535
4.03 (-0.0036)	-20817	-20918	-20919	-20840	-20881	-20881	-20852	-20862	-20862
4.34 (-0.0048)	-21049	-21146	-21146	-21070	-21108	-21108	-21080	-21089	-21089
4.65 (-0.0060)	-21212	-21303	-21304	-21229	-21265	-21266	-21237	-21246	-21246
4.96 (-0.0048)	-3219	-3290	-3290	-3262	-3290	-3290	-3283	-3290	-3290
5.27 (-0.0036)	10809	10771	10771	10768	10753	10752	10747	10743	10743
5.58 (-0.0024)	14427	14481	14481	14425	14447	14447	14424	14429	14429
5.89 (-0.0012)	15801	15890	15891	15819	15855	15855	15828	15837	15837
6.20 (0.0)	16783	16889	16890	16810	16853	16853	16824	16835	16835

Table III(c) continued

Stress (psi) Time (strain)	$\Delta t = 0.0025$			$\Delta t = 0.001$			$\Delta t = 0.00025$		
	Euler	Modified Euler	Runge Kutta	Euler	Modified Euler	Runge Kutta	Euler	Modified Euler	Runge Kutta
6.51 (0.0012)	17492	17603	17604	17522	17567	17567	17537	17548	17548
6.82 (0.0024)	17998	18108	18109	18027	18071	18071	18041	18052	18052
7.13 (0.0036)	18356	18462	18462	18382	18424	18424	18395	18405	18405
7.44 (0.0048)	18608	18707	18708	18630	18670	18670	18641	18651	18651
7.75 (0.0060)	18784	18878	18878	18803	18840	18840	18812	18821	18821
8.06 (0.0048)	793	866	866	838	867	867	859	867	867
8.37 (0.0036)	-13233	-13192	-13192	-13190	-13174	-13174	-13169	-13165	-13165
8.68 (0.0024)	-16844	-16896	-16896	-16841	-16862	-16862	-16839	-16845	-16845
8.99 (0.0012)	-18213	-18301	-18301	-18230	-18265	-18265	-18239	-18248	-18248
9.30 (0.0)	-19192	-19296	-19297	-19218	-19260	-19260	-19232	-19242	-19242
9.61 (-0.0012)	-19897	-20008	-20008	-19927	-19971	-19971	-19942	-19953	-19953
9.92 (-0.0024)	-20401	-20510	-20511	-20429	-20473	-20473	-20443	-20453	-20454
10.23 (-0.0036)	-20757	-20862	-20863	-20783	-20825	-20825	-20795	-20806	-20806
10.54 (-0.0048)	-21008	-21107	-21107	-21030	-21069	-21069	-21040	-21050	-21050
10.85 (-0.0060)	-21183	-21276	-21277	-21201	-21238	-21239	-21210	-21219	-21219
11.16 (-0.0048)	-3192	-3264	-3265	-3236	-3265	-3265	-3258	-3265	-3265
11.47 (-0.0036)	10835	10795	10795	10793	10777	10777	10772	10768	10768
11.78 (-0.0024)	14448	14499	14500	14444	14465	14465	14442	14448	14448
12.09 (-0.0012)	15816	15904	15905	15833	15869	15869	15842	15851	15851
12.40 (0.0)	16794	16899	16900	16821	16863	16863	16834	16845	16845
12.71 (0.0012)	17500	17610	17611	17530	17574	17574	17544	17555	17555
13.02 (0.0024)	18004	18113	18114	18032	18076	18076	18046	18057	18057
13.33 (0.0036)	18360	18465	18466	18386	18428	18428	18398	18409	18409
13.64 (0.0048)	18611	18710	18710	18633	18672	18673	18643	18653	18653
13.95 (0.0060)	18786	18879	18880	18805	18842	18842	18813	18823	18823

Table IV(a)

Values of stress at different times obtained using the integration strategies proposed (i) by Kumar et al. and (ii) in the present report, for Bodner-Partom Model

Time (sec.) \ Stress (KSI)	Kumar et al.	Accurate Values*	Time (sec.) \ Stress (KSI)	Present Report	Accurate Values*
5.0	93.73	93.72	5.11	95.78	95.78
10.06203	149.34	149.30	10.01	149.18	149.17
15.26203	156.51	156.42	15.01	156.29	156.27
20.14203	157.85	157.80	20.13	157.80	157.79
25.0	158.06	158.05	25.00	158.05	158.05
30.0	54.67	60.06	32.265	17.58	17.60
35.0	-39.05	-33.66	37.385	-78.39	-78.36
40.0	-132.76	-127.37	40.025	-127.87	-127.83
45.0	-157.97	-157.93	45.145	-157.94	-157.94
50.0	-158.08	-158.07	50.00	-158.07	-158.07
55.25	-139.86	-140.58	55.04	-140.78	-140.80
60.25	-136.57	-137.01	60.00	-137.12	-137.14
65.25	-134.60	-134.92	65.12	-134.95	-134.97
70.25	-133.20	-133.45	70.24	-133.44	-133.45
75.00	-132.16	-132.37	75.00	-132.35	-132.37
80.00	-38.33	-38.60	80.92	-21.33	-21.36
85.00	55.39	55.11	86.04	74.63	74.61
90.00	148.03	147.49	90.00	147.54	147.49
95.1875	157.90	157.88	95.14	157.88	157.87
100.0	158.07	158.06	100.00	158.06	158.06

\* defined in Section 3.1.

$$e_{\min} = 10^{-4}, e_{\max} = 10^{-3} \text{ and } Tol_l = 10^{-5}, Tol_u = 10^{-4}$$

Table IV(b)

Values of non-dimensional stress at different times obtained using the integration strategies proposed (i) by Kumar et al. and (ii) present report, for Robinson Model

Stress Time	Kumar et al.	Accurate Values	Stress Time	Present Report	Accurate Values
0.001000582	7.842	7.839	0.001	7.841	7.839
0.002002582	9.714	9.712	0.002008	9.720	9.718
0.003010582	10.704	10.701	0.003	10.694	10.692
0.004018582	11.469	11.465	0.004024	11.472	11.469
0.005	12.098	12.094	0.005	12.096	12.094
0.006183284	-0.665	-0.631	0.006018	1.012	1.011
0.00700570	-7.400	-7.362	0.0070039	-7.390	-7.361
0.008005702	-9.577	-9.569	0.00799987	-9.569	-9.562
0.009013514	-10.607	-10.601	0.00900787	-10.601	-10.598
0.01001351	-11.384	-11.377	0.01001587	-11.385	-11.379
0.01101351	-12.036	-12.029	0.01100787	-12.031	-12.026
0.01202914	-12.614	-12.608	0.01199987	-12.597	-12.592
0.01302914	-13.125	-13.118	0.01299817	-13.105	-13.103
0.01399789	-13.575	-13.569	0.01401587	-13.581	-13.576
0.015	-14.005	-13.997	0.015	-14.002	-13.997
0.0160298	-2.764	-2.774	0.016026	-2.815	-2.812
0.01700214	6.342	6.332	0.01700384	6.346	6.343
0.01800214	9.320	9.314	0.01799984	9.312	9.311
0.01900214	10.428	10.423	0.01900784	10.429	10.428
0.02000214	11.240	11.235	0.02001584	11.247	11.244
0.02101777	11.922	11.916	0.02100784	11.913	11.910
0.02201777	12.505	12.499	0.02199984	12.494	12.489
0.02301777	13.026	13.020	0.02299184	13.010	13.007
0.02401777	13.499	13.492	0.02401584	13.495	13.491
0.025	13.926	13.918	0.025	13.922	13.918

Table IV(b) - continued

Stress Time	Kumar et al.	Accurate Values	Stress Time	Present Report	Accurate Values
0.02617414	1.192	1.253	0.026026	2.735	2.734
0.02700169	-6.439	-6.382	0.02700172	-6.384	-6.382
0.0290056	-9.344	-9.330	0.02800572	-9.332	-9.330
0.0290056	-10.443	-10.433	0.02899772	-10.428	-10.427
0.0300056	-11.252	-11.243	0.03000572	-11.245	-11.244
0.03102123	-11.933	-11.923	0.03102972	-11.931	-11.928
0.03200365	-12.505	-12.496	0.03202172	-12.508	-12.505
0.03300365	-13.025	-13.016	0.03304572	-13.040	-13.037
0.03400365	-13.499	-13.489	0.03400572	-13.494	-13.490
0.035	-13.931	-13.922	0.035	-13.923	-13.922
0.0364051	1.153	1.035	0.036026	-2.739	-2.737
0.03700267	6.451	6.385	0.03700172	6.382	6.379
0.03800267	9.344	9.326	0.03800572	9.331	9.330
0.03900267	10.443	10.430	0.03901372	10.442	10.440
0.04000267	11.252	11.240	0.04000572	11.245	11.243
0.0410183	11.933	11.921	0.04102972	11.931	11.928
0.04200658	12.508	12.497	0.04202172	12.508	12.505
0.04300658	13.028	13.017	0.04304572	13.040	13.037
0.04400658	13.501	13.490	0.04400572	13.493	13.490
0.045	13.933	13.922	0.045	13.925	13.922

$e_{\min} = 10^{-5}$  ,  $e_{\max} = 10^{-4}$  and  $Tol_l = 10^{-6}$  ,  $Tol_u = 10^{-5}$  .

Table IV(c)

Values of stress (psi) at different times (sec.) obtained using the integration strategies proposed (i) by Kumar et al. and (ii) in present report for Walker Model

Stress Time (psi) (sec.)	Kumar et al. Accurate Values	Stress Time (psi) (sec.)	Present Report	Accurate Values
0.3102109	13795	0.31	13890	13791
0.6208359	16717	0.62	16737	16710
0.9302109	17487	0.93	17501	17479
1.240211	18008	1.24	18021	18000
1.55	18373	1.55	18386	18365
1.885252	-878	1.86	364	434
2.170216	-13599	2.17	-13717	-13574
2.481074	-17157	2.48	-17185	-17149
2.79	-18472	2.79	-18487	-18462
3.10129	-19405	3.10	-19410	-19390
3.412596	-20070	3.41	-20071	-20052
3.720309	-20533	3.72	-20539	-20520
4.026825	-20857	4.03	-20868	-20845
4.342920	-21088	4.34	-21098	-21076
4.65	-21243	4.65	-21257	-21235
4.96674	-2913	4.975	-2430	-2508
5.270131	10788	5.27	10909	10754
5.582631	14447	5.58	14461	14424
5.892006	15845	5.89	15849	15825
6.201381	16838	6.20	16839	16820
6.511439	17549	6.51	17550	17532
6.821596	18052	6.82	18055	18037
7.130971	18403	7.13	18410	18391
7.443471	18650	7.44	18659	18637

Table IV(c) - continued

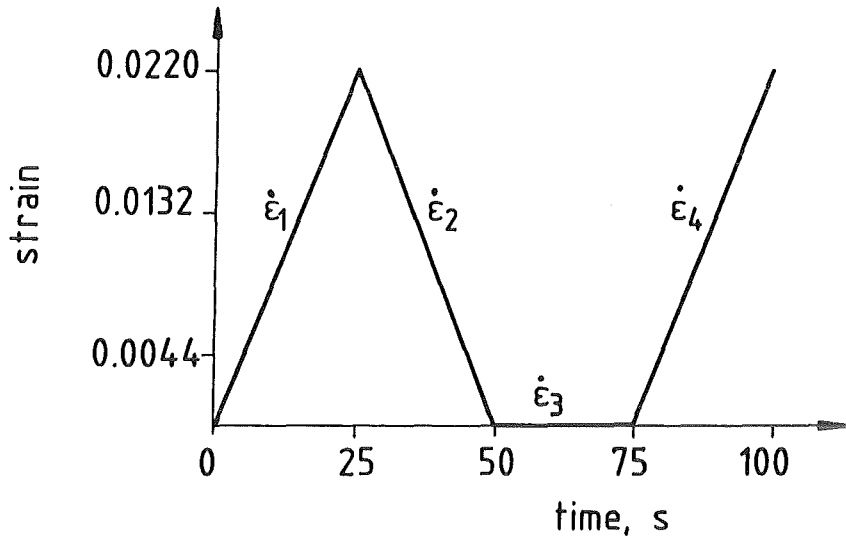
Time (sec.)	Stress (psi)	Kumar et al. Accurate Values	Time (sec.)	Stress (psi)	Present Report Accurate Values
7.75		18817 18809	7.75		18832 18809
8.068649		394 409	8.08		-244 -172
8.371330		-13229 -13210	8.37		-13347 -13176
8.680473		-16847 -16840	8.68		-16876 -16840
8.992973		-18256 -18247	8.99		-18259 -18236
9.302348		-19246 -19233	9.30		-19246 -19227
9.611723		-19953 -19939	9.61		-19954 -19937
9.921098		-20453 -20440	9.92		-20457 -20439
10.23360		-20806 -20794	10.23		-20810 -20791
10.55235		-21055 -21044	10.54		-21058 -21037
10.85		-21217 -21207	10.85		-21230 -21207
11.18375		-1986 -2034	11.175		-2404 -2482
11.47054		10838 10793	11.47		10935 10779
11.78018		14454 14444	11.78		14480 14443
12.09489		15871 15859	12.09		15863 15839
12.40072		16847 16830	12.40		16849 16830
12.71086		17556 17540	12.71		17557 17539
13.02114		18057 18043	13.02		18060 18042
13.3333		18409 18397	13.33		18414 18394
13.64295		18652 18641	13.64		18661 18640
13.95		18819 18810	13.95		18833 18810

$e_{\min} = 10^{-5}$ ,  $e_{\max} = 10^{-4}$  and  $Tol_1 = 10^{-5}$ ,  $Tol_u = 10^{-4}$ .

Table V

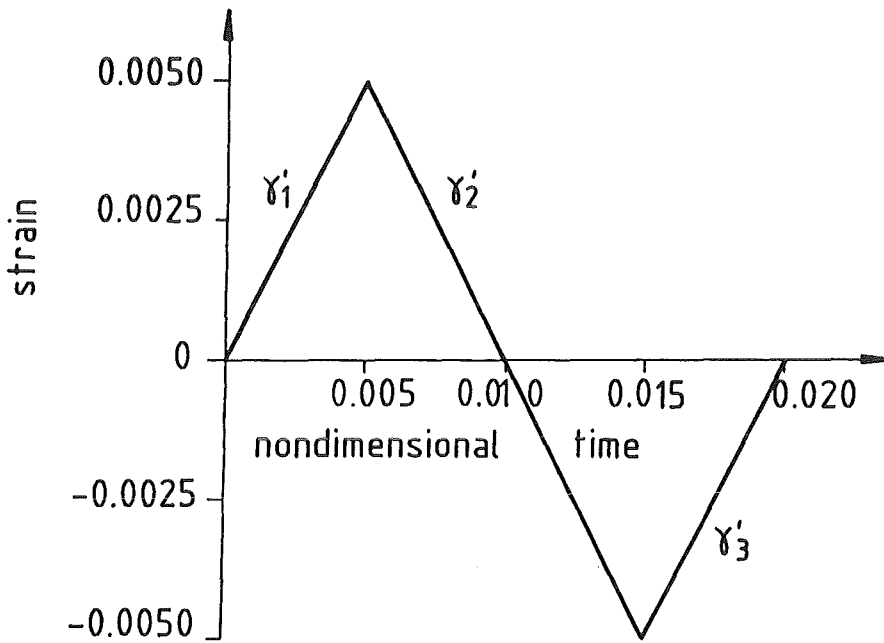
Comparison of Error Norms and CPU-Times for Kumar et al. and Present Integration Strategies in Case of Different Viscoplastic Models.

Model	Strategy	Error Norms		CPU - Time (secs.)
		Complete Cycles	Peak Values	Complete Cycles
BODNER	Kumar et al.	0.1887	$3 \times 10^{-7}$	0.55
	Present	0.00225	$2 \times 10^{-8}$	0.16
ROBINSON	Kumar et al.	0.0543	$2 \times 10^{-6}$	0.63
	Present	0.0045	$5 \times 10^{-7}$	0.48
WALKER	Kumar et al.	0.0498	$1.0 \times 10^{-6}$	0.51
	Present	0.4517	$0.67 \times 10^{-5}$	0.76



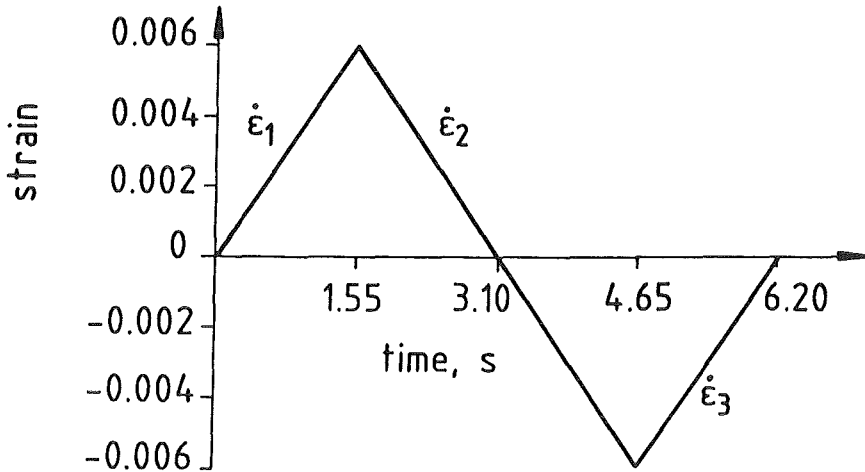
$$\begin{aligned} \dot{\epsilon}_1 &= 8.8 \times 10^{-4} \text{ s}^{-1} \\ &\quad (25 \text{ s}) \\ \dot{\epsilon}_2 &= -8.8 \times 10^{-4} \text{ s}^{-1} \\ &\quad (25 \text{ s}) \\ \dot{\epsilon}_3 &= 0.0 \text{ (25 s)} \\ \dot{\epsilon}_4 &= \dot{\epsilon}_1 \text{ (25 s)}. \end{aligned}$$

a) Bodner - Partom Model (Ref. [34]).



$$\begin{aligned} \gamma'_1 &= 1.0 \text{ (0.005 units)} \\ \gamma'_2 &= 1.0 \text{ (0.010 units)} \\ \gamma'_3 &= \gamma'_1 \text{ (0.005 units)}. \end{aligned}$$

b) Robinson Model (Ref. [4])



$$\begin{aligned} \dot{\epsilon}_1 &= 3.87 \times 10^{-3} \text{ s}^{-1} \text{ (1.55 s)} \\ \dot{\epsilon}_2 &= 3.87 \times 10^{-3} \text{ s}^{-1} \text{ (3.10 s)} \\ \dot{\epsilon}_3 &= \dot{\epsilon}_1 \text{ (1.55 s)}. \end{aligned}$$

c) Walker Model (Ref. [6])

Fig. 1 Cyclic loadings for different models.

### Bodner - Partom Model

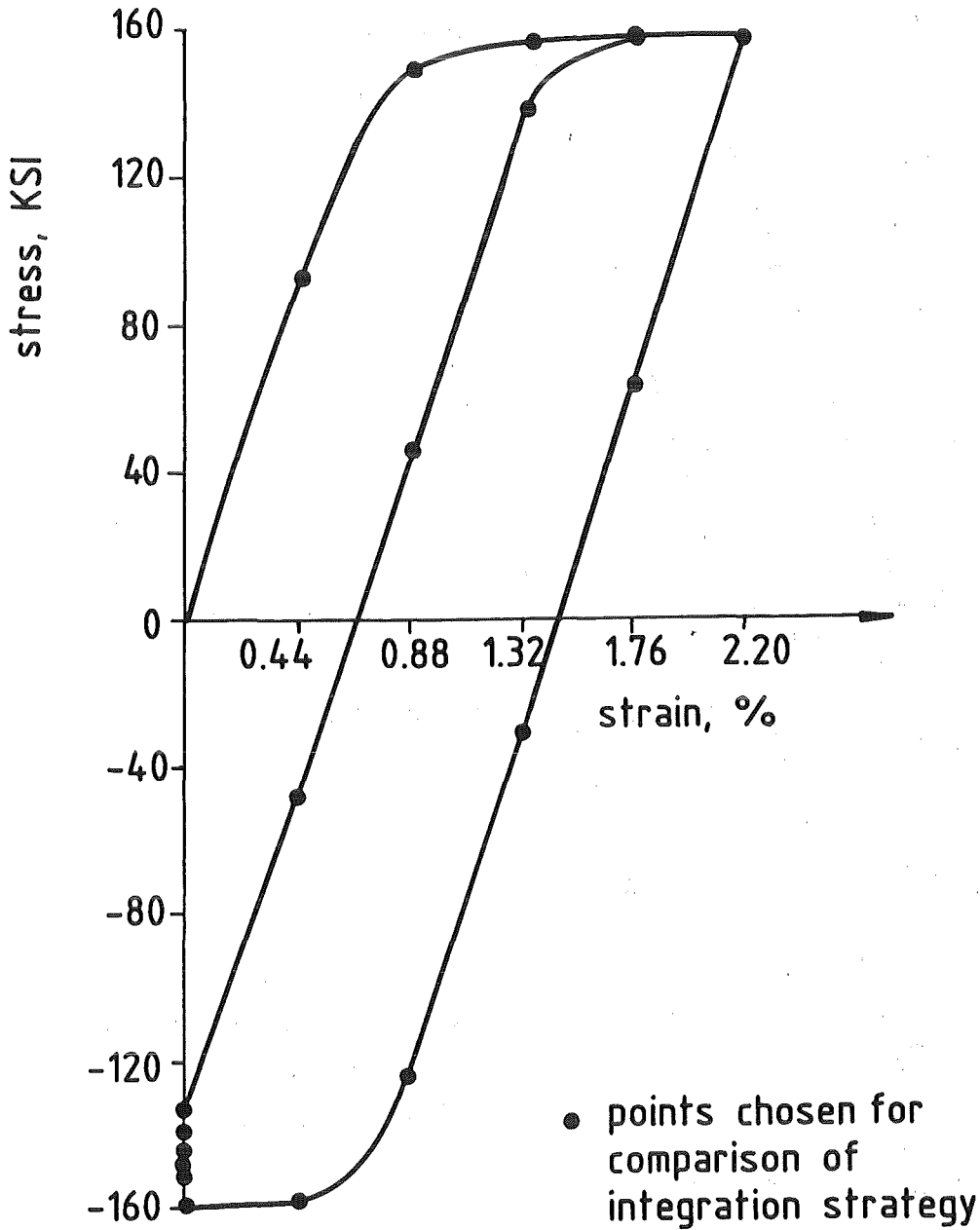


Fig. 2 a: Stresses (accurate) vs strain for Bodner -Partom model (one cycle) - KUMAR et al. STRATEGY.

### Bodner - Partom Model

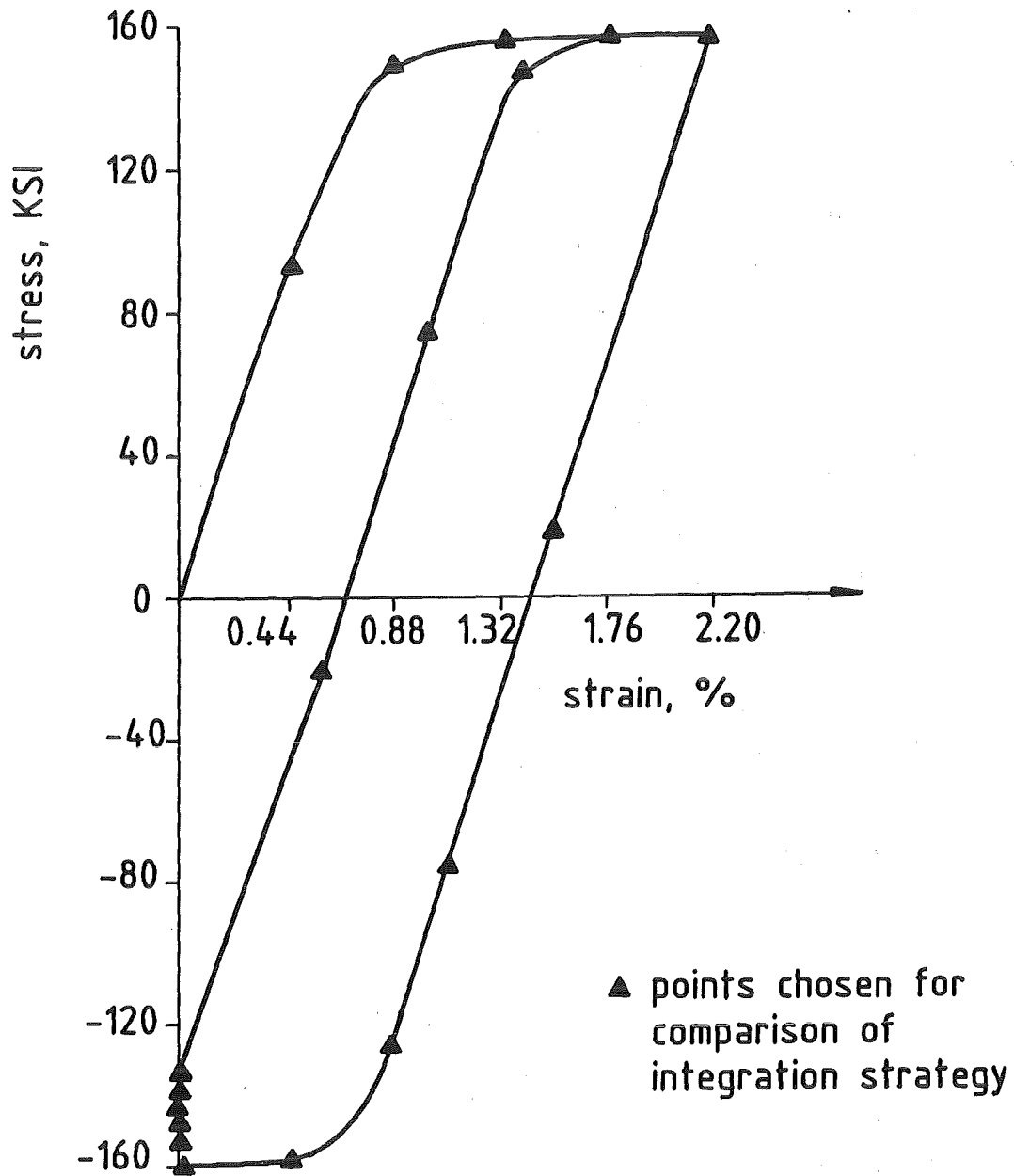


Fig. 2 b: Stresses (accurate) vs strain for Bodner-Partom model (one cycle) - PRESENT STRATEGY.

### Robinson Model

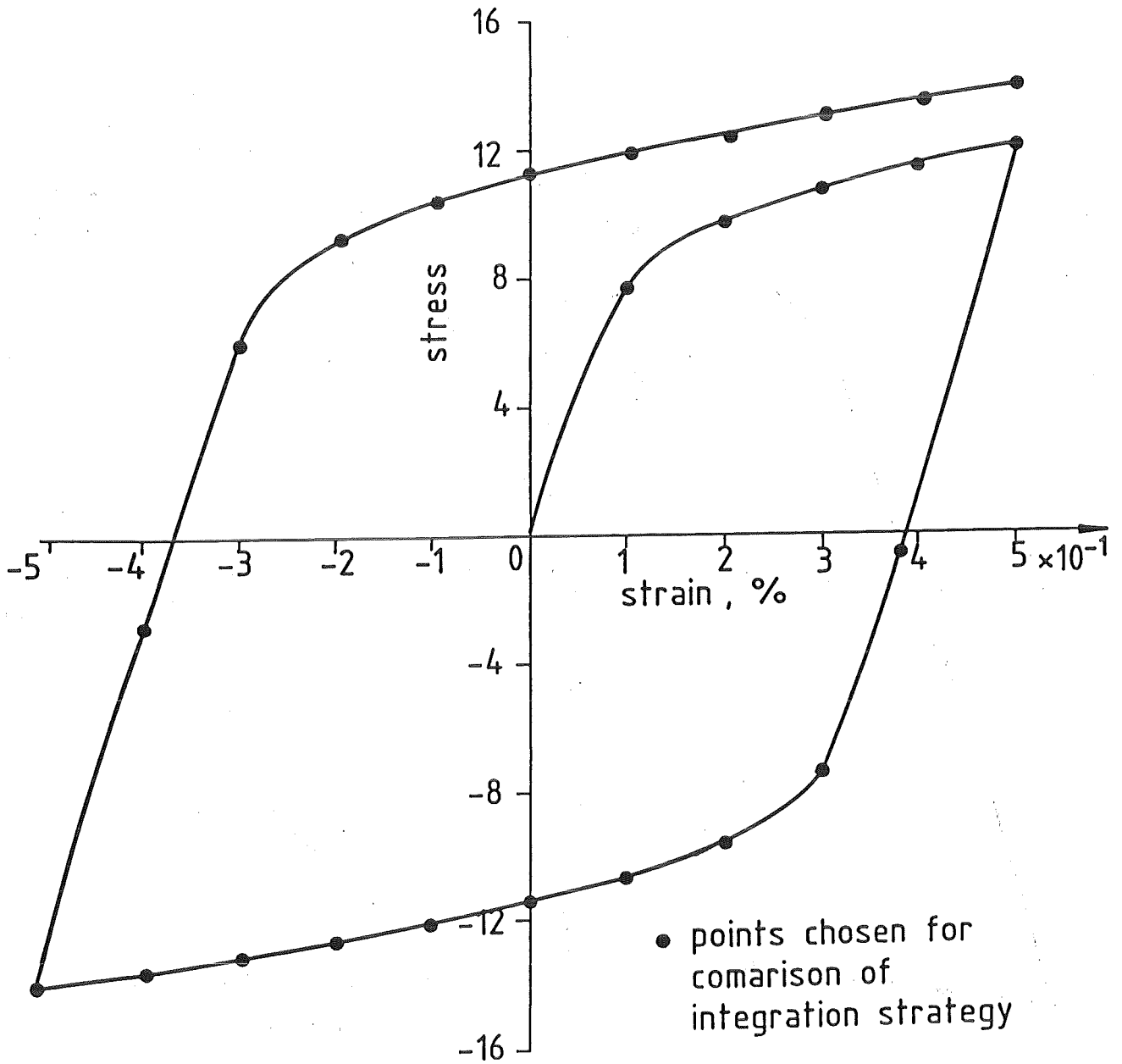


Fig. 3a: Stress (nondimensional) vs strain for Robinson model (one and one-quarter of a cycle) - KUMAR et al. STRATEGY,

### Robinson Model

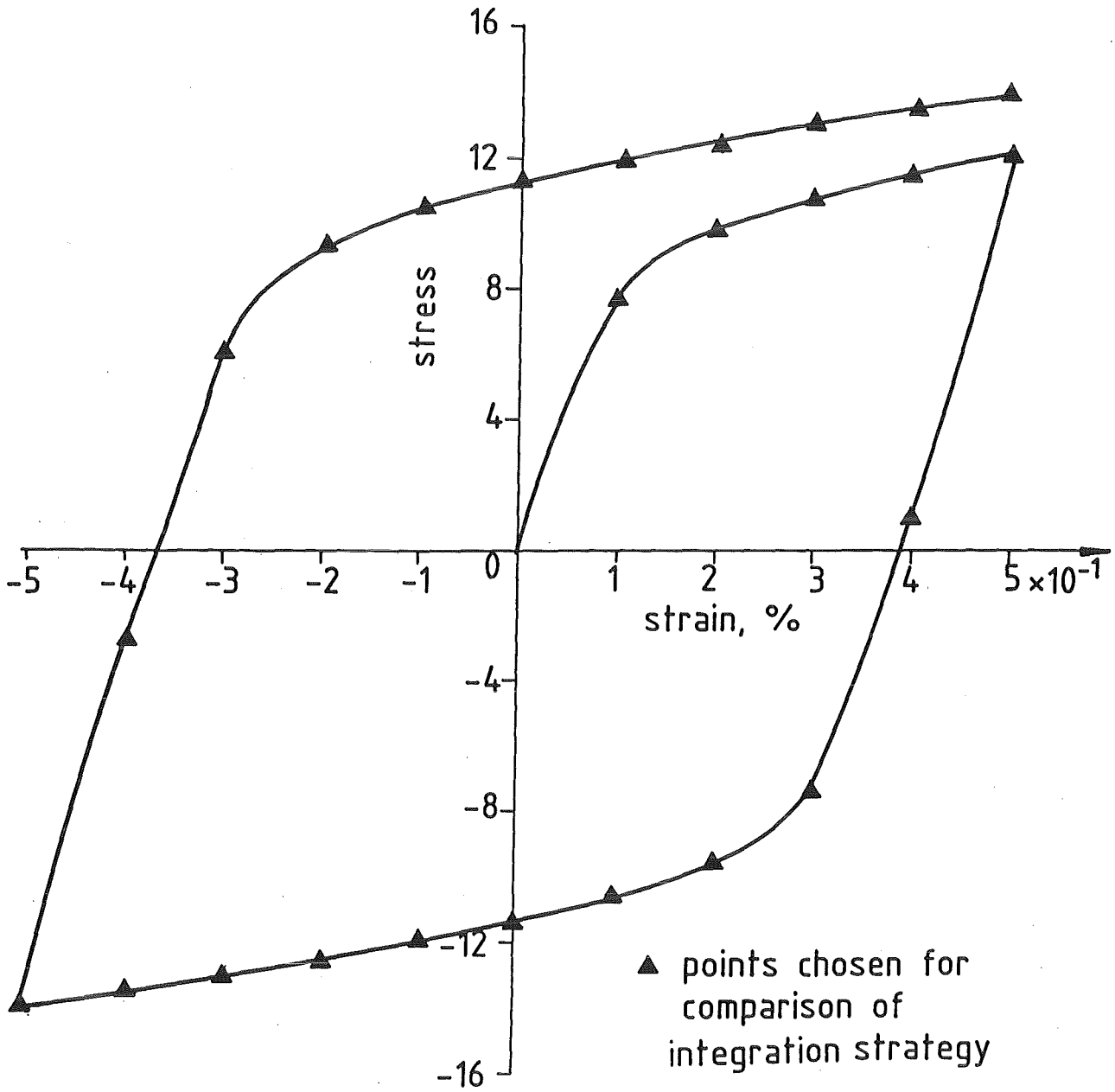


Fig. 3b: Stress (nondimensional) vs strain for Robinson model (one and one-quarter of a cycle) - PRESENT STRATEGY.

### Walker Model

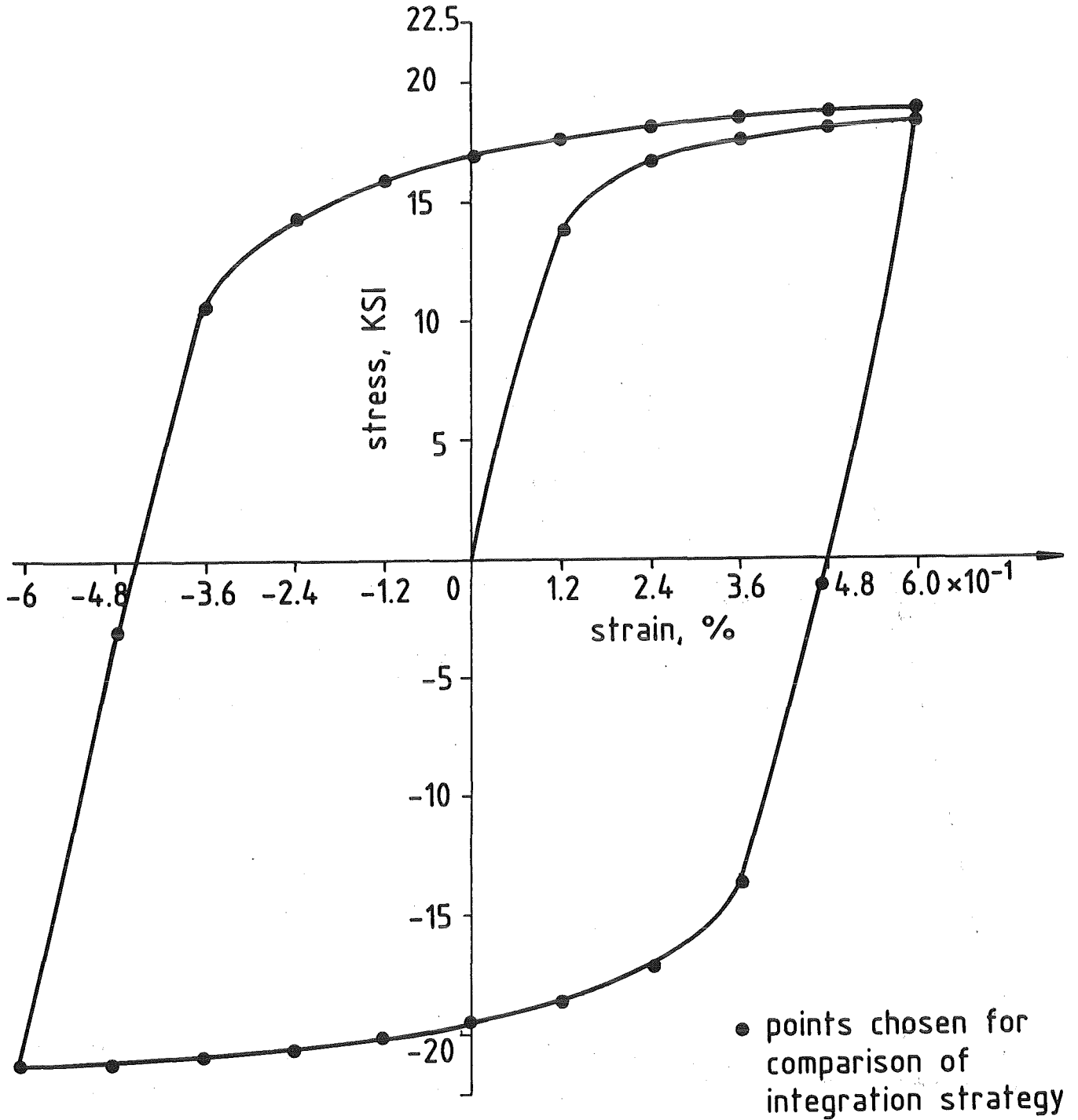


Fig. 4 a: Stress vs strain for Walker model (one and one-quarter of a cycle) - KUMAR et al. STRATEGY.

### Walker Model

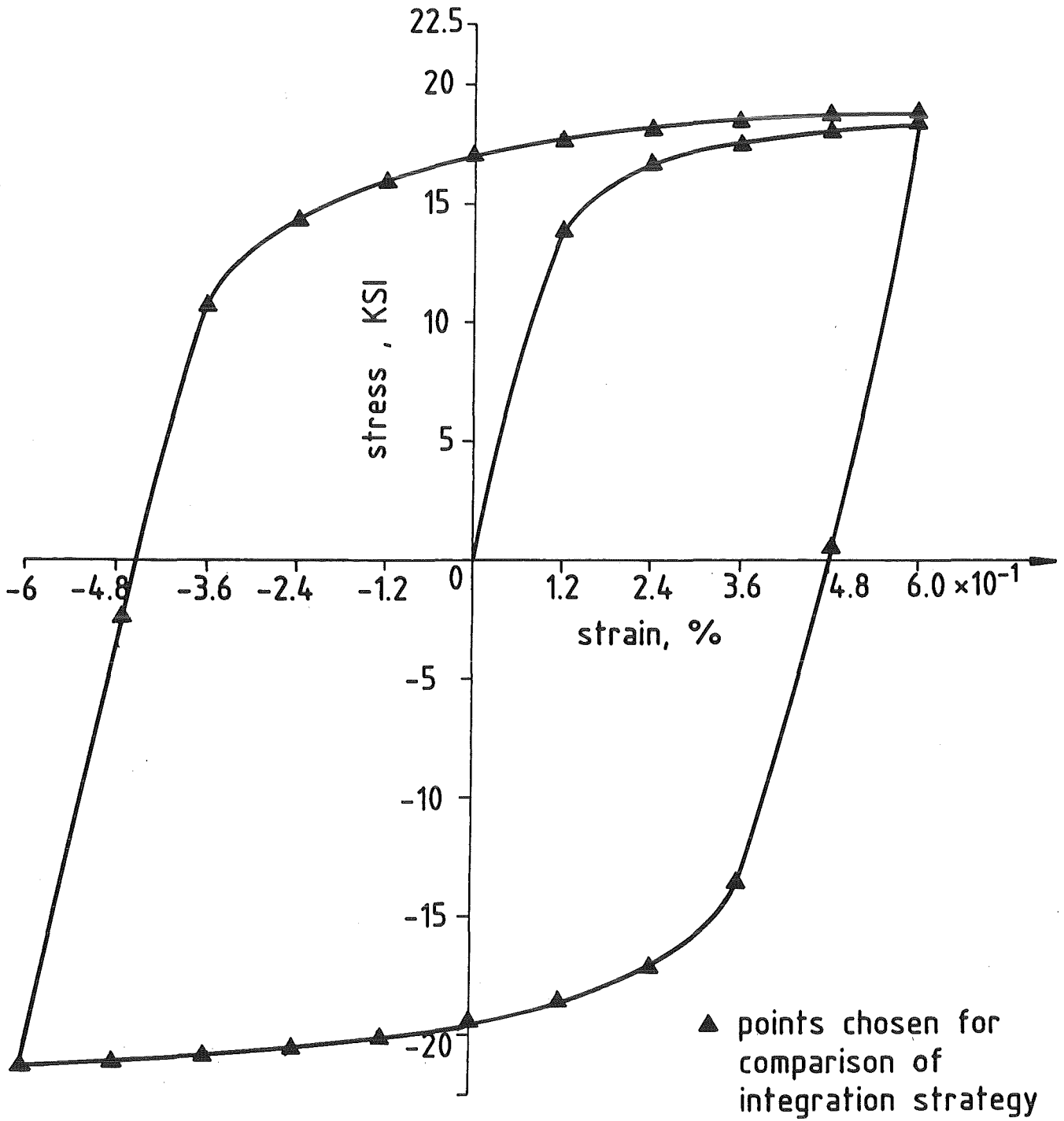


Fig. 4 b: Stress vs strain for Walker model (one and one-quarter of a cycle) - PRESENT STRATEGY.